Acta Mechanica Sinica (2021) 37(2):201–217
https://doi.org/10.1007/s10409-021-01057-3

REVIEW

Mechanotransduction of liver sinusoidal endothelial cells under varied mechanical stimuli

Xinyu Shu[1,2] · Ning Li[1,2] · Yi Wu[1,2] · Wang Li[1,2] · Xiaoyu Zhang[1,2] · Peiwen Li[1] · Dongyuan Lü[1,2] · Shouqin Lü[1,2] · Mian Long[1,2]

Received: 31 August 2020 / Revised: 14 December 2020 / Accepted: 5 January 2021 / Published online: 10 March 2021

Abstract

Liver sinusoidal endothelial cells (LSECs) are the gatekeeper of liver to maintain hepatic homeostasis. They are formed into the highly specialized endothelium between vascular lumen and the space of Disse and are mechanosensitive to respond varied microenvironments. Shear stress and mechanical stretch induced by blood perfusion and substrate stiffness enhancement derived from deposition of extracellular matrix (ECM) are major mechanical stimuli that surround LSECs. This review introduces how LSECs respond to the external forces in both physiological and pathological cases and what is the interplay of LSECs with other hepatic cells. Molecular mechanisms that potentiate LSECs mechanotransduction are also discussed.

Keywords Liver sinusoidal endothelial cell · Shear stress · Mechanical stretch · Extracellular matrix · Stiffness

Abbreviations

AFM	Atomic force microscopy
ARFI	Acoustic radiation force impulse imaging
BMP	Bone morphogenic protein
BMSC	Bone marrow stromal cell
CFD	Computational fluid dynamics
CH	Congestive hepatopathy
CT	Computed tomography
Dnmt3b	DNA methyltransferase 3b
ECM	Extracellular matrix
eNOS	Endothelial nitric oxide synthase
EVG	Elastica van Gieson
F-actin	Filamentous actin
HCV	Hepatitis C virus
HGF	Hepatocyte growth factor
Hh	Hedgehog
HLH	Helix–loop–helix
HSC	Hepatic stellate cell
HUVEC	Human umbilical vein endothelial cell
IAA	Iodoacetic acid
Id1	Inhibitor of DNA binding 1
Ihh	Indian hedgehog
I/R	Ischemia-reperfusion
KLF2	Kruppel-like factor 2
LOX	Lysyl oxidase
LPA	Lysophosphatidic acid
LSEC	Liver sinusoidal endothelial cell
LXRα	Liver X receptor α
MEC	Mammary epithelial cell
MMP9	Matrix metalloproteinase-9
MRE	Magnetic resonance elastography
MSC	Mesenchymal stem cell
NAFLD	Nonalcoholic fatty liver disease
NECD	Notch extracellular domain
NETs	Neutrophil extracellular traps
NICD	Notch intracellular domain
NO	Nitric oxide
NRP1	Neuropilin-1
PH	Partial hepatectomy
pIVCL	Partial inferior vena cava ligation
PVE	Portal vein embolization
ROS	Reactive oxygen species
RPM	Revolutions per minute

Executive Editor: Xi-Qiao Feng

✉ Ning Li
lining_1@imech.ac.cn

✉ Mian Long
mlong@imech.ac.cn

[1] Center for Biomechanics and Bioengineering, Key Laboratory of Microgravity (National Microgravity Laboratory), and Beijing Key Laboratory of Engineered Construction and Mechanobiology, Institute of Mechanics, Chinese Academy of Sciences, Beijing 100190, China

[2] School of Engineering Sciences, University of Chinese Academy of Sciences, Beijing 100049, China

Shh	Sonic hedgehog
SMC	Smooth muscle cell
TG	Transglutaminase
TM	Thrombomodulin
UTE	Ultrasound-based technique of transient elastography
VEGFR2	Vascular endothelial cell growth factor receptor 2
VEGFR3	Vascular endothelial cell growth factor receptor 3
YAP	Yes-associated protein

1 Introduction

1.1 Liver sinusoidal endothelial cells

Liver sinusoidal endothelial cells (LSECs) are the maximized population of non-parenchymal hepatic cells up to 15% to 20% [1, 2] with a tiny total volume fraction of only 3% [2]. They are quite thin endothelial cells lining along liver sinusoids, making up a complex microvascular bed and receiving a dual blood supply of 70% from the portal vein and 30% from the hepatic artery [3]. Unlike other endothelial cells, LSECs are highly specialized cells with a unique structure called "fenestrae" [4] that are permeable pores fused by luminal and abluminal plasma membrane, providing open channels for mass transfer between the sinusoid and the space of Disse [5]. Fenestrae usually range from 50 to 200 nm in diameter [6] and are grouped into organized sieve plates [7] (Fig. 1).

LSECs play an indispensable role as a gatekeeper to retain hepatic homeostasis, especially participating in metabolism, inflammation and regeneration [8–10]. They are also functional in sinusoidal crosstalk with other liver cells to regulate the hepatic microenvironment [9]. The preservation of fenestrae structure is necessary for LSECs to maintain normal physiological state [1]. Fenestrae are able to contract or dilate in response to the alterations of sinusoidal blood flow and perfusion pressure [11]. Loss of fenestrae, also known as "capillarization", implies the disappearance of their unique and specialized phenotype [12] and the changes in function, which is believed to precede the development of abundant chronic liver diseases [13, 14] and acute liver injuries [1]. Evidently, LSECs are critical for various pathological processes and it is key to understand their functions and explore their dedifferentiation. To date, researches are mainly focused on those biochemical factors that regulate LSECs [15], while mechanical microenvironment is much less discussed but matters a lot.

1.2 Mechanical microenvironment of LSECs in vivo

LSECs are located in a complicated mechanical microenvironment due to the intricate microstructures and specialized dual blood supply system in liver [16]. Physiologically, the amount of hepatic blood flow ranges from 800 to 1200 $mL{\cdot}min^{-1}$ [17]. When the blood enters liver sinusoids, the flow rate is greatly influenced by localized biochemical and biomechanical factors. Liver microvasculature consists of long, straight sinusoids at a length of 250 μm with short interconnecting sinusoids, and their diameters increase from 7 μm in the periportal to 15 μm

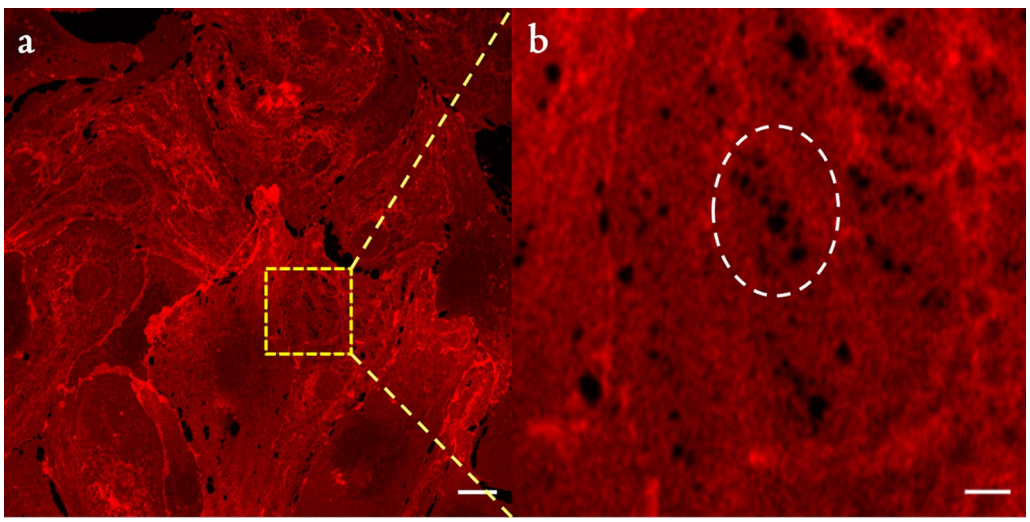

Fig. 1 Morphology of primary isolated mice liver sinusoidal endothelial cells (LSECs). **a** Representative fluorescent image of primary C57BL/6 mice LSECs, recorded at $\lambda_{Exc}/\lambda_{Em}$: 633 nm to 654 nm, labelled by cellmask™ Plasma Membrane Stains (scale bar: 10 μm). **b** Enlarged view of the yellow box area on the left. White cycle indicates the fenestrae lumped into sieve plates (scale bar: 2 μm)

in the pericentral region [11]. This irregular structure complicates the perfusion of blood flow in liver. Moreover, hepatic macrophages, Kupffer cells, attach onto the endothelium and protrude into sinusoids, serving as an obstacle to flow [11] that further enhances the complexity. Under normal conditions, LSECs can release vasodilators to counteract the upregulation of shear stress in order to balance blood pressure [1]. LSECs also inhibit the activation of hepatic stellate cells (HSCs) through a paracrine pathway, thus maintaining a relative small quantity of ECM [1].

In pathological cases, these mechanical factors in liver sinusoids turn to be remarkably different. During liver operation, the interruption of irrigation is required to prevent possible bleeding by suspending blood flow for a period of time [18]. A partial hepatectomy (PH) surgery leads to the increased blood perfusion, resulting in immediately higher portal flow and wider vessel diameters [19, 20]. Chronic liver diseases including hepatic fibrosis and cirrhosis bring about the capillarization of LSECs [1], reducing the infiltration from the sinusoids to the space of Disse via the loss of fenestrae. And the capillarized LSECs allow the activation of HSCs to produce massive collagens [21] and promote the vasoconstriction to increase intrahepatic resistance [22] or even induce portal hypertension. These processes are always accompanied by angiogenesis in liver [23], enabling the microvasculature network to be further extended and complicated. On the other hand, the excessive ECM produced by activated HSCs are deposited and cross-linked in the space of Disse, which hardens the liver organ than the healthy one [16]. The shear storage modulus measured by rheometry is approximately 400 Pa for a normal rat liver but rises to 1.2–1.4 kPa for a fibrotic one induced by carbon tetrachloride [24]. In fact, all kinds of causes that induce liver fibrosis could enhance the liver stiffness, including nonalcoholic fatty liver disease (NAFLD) [25], autoimmune hepatitis [26], and hepatitis virus [27]. For example, a 15% increase in liver stiffness of NAFLD patients, measured by MRE, is associated with fibrotic progression and implies the transformation from early to advanced fibrosis [25]. And those chronic liver diseases, including NAFLD and virus infection, can also induce the liver fibrosis where the stiffness ranges from F0 (< 7.1 kPa) to F4 (> 12.5 kPa) stage [28, 29]. Thus, the alterations of mechanical microenvironment in liver tissue generally appear during different pathological and developmental stages of hepatic diseases.

To elaborate the mechanical microenvironment LSECs reside, here we mainly focus on the effects of blood flow and ECM-dependent stiffness. We attempt to introduce the physical principles of shear stress, mechanical stretch and substrate stiffness on LSECs, and also summarize the related biomechanical measurement and biochemical functions. In addition, several potential mechanosensitive molecules are discussed to understand the underlying mechanotransduction.

2 Shear stress on LSECs

2.1 Physical principles

Forces produced by blood flow on vessels can be divided into two vectors: one is perpendicular to the wall to create blood pressure, and the other is parallel to the vessel to induce shear stress (Fig. 2). Shear stress is a kind of frictional force acting on the apical surface of endothelial cells by blood flow. It is determined by the fluid viscosity, mean fluid flow rate, and the physical radius of blood vessels [30, 31]. For a flow of Newtonian fluid in a long, straight tube, the shear stress τ is given by Poiseuille's law,

$$\tau = \frac{4\mu Q}{\pi r^3}, \tag{1}$$

where Q is the flow rate, μ is the fluid viscosity, and r is the tube radius. It is noticed that blood flow dynamics in liver sinusoids is much complicated mainly due to vascular permeability induced by LSEC fenestrae.

2.2 Shear stress measurements

To date, the accurate values of shear stresses in liver sinusoids have not been directly measured in either human species or animal models. Since the dimension of liver sinusoids is very small even in large-sized animals like swine [32] and also varies from one to another sinusoid in the liver, it is difficult to determine the exact values. In addition, fluid viscosity inside sinusoids can hardly be evaluated accurately since it changes with hemodilution [1, 16].

Historically, an electromagnetic flowmeter was used to determine portal hemodynamics in liver as early as 1956 [33]. The electromagnetic flowmeter is a flow sensor with a tube made by non-magnetizable metal and inner lining of electrical-insulating material. Voltage is induced by the flow of the conductive liquid and the output voltage signals are collected to estimate the flow rate. This flowmeter is used in rat liver to measure portal vein flow in cirrhosis and the shear stress is calculated by Eq. (1) on portal flow rate, blood viscosity, and portal vein radius. Data indicate that the shear stress of the portal vein is decreased with the development of hepatic fibrosis, especially during venous remodeling [34]. Nevertheless, it is still difficult to estimate the shear stress in a liver sinusoid either.

Computational fluid dynamics (CFD) is one of theoretical approaches to predict the flow features based on conservation laws [35, 36]. With the techniques of vascular corrosion

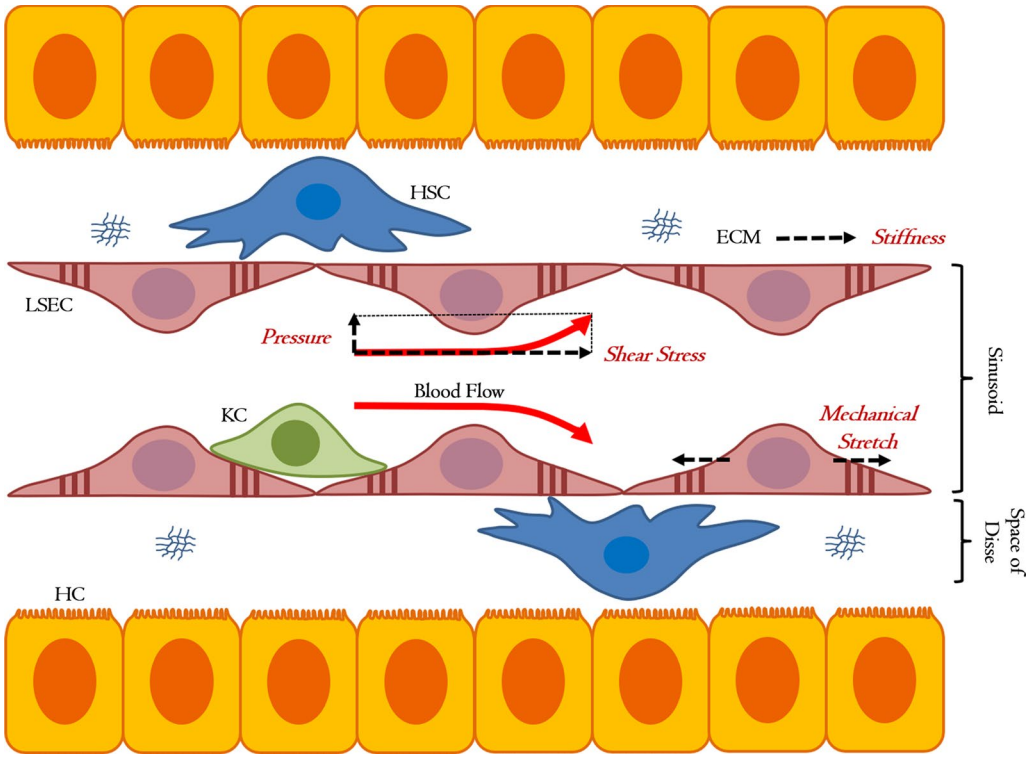

Fig. 2 Mechanical microenvironment of LSECs. LSECs, lining along the hepatic capillaries, separate the sinusoids and the space of Disse. Blood perfusion and extracellular matrix (ECM) stiffness are two main sources of mechanical stimuli for LSECs. The parallel vector of blood flow induces shear stress while the perpendicular one creates pressure on LSECs. And ECM derived from hepatic stellate cells (HSCs) serves as the major source of substrate stiffness that LSECs can sense

casting and micro-computed tomography (CT) imaging, the perfusion characteristics in liver can be simulated using CFD. These simulations predict that the wall shear stress of hepatic sinusoids yields below 1 Pa and rises up when the sinusoidal lumen is narrowed down, presenting very low shear onto most surfaces of LSECs [37]. CFD is also used in liver cirrhosis models to deduce lower shear stress and higher probability of disturbed flow compared with normal liver, suggesting the appearance of portal vein thrombosis [38] and also quantifying the perfusion characteristics of the cirrhotic microcirculation [39]. Besides, three-dimensional (3D) CFD models are developed to compare flow dynamics of hepatic lobules among normal, fibrotic and cirrhotic livers [40]. Evidently, applying the CFD approach alone is insufficient to determine actual shear stresses of sinusoids in vivo.

2.3 Responses to shear stress

LSECs act as a regulator of vascular tone in liver. Under physiological conditions, they sense the changes in blood flow and release vasoactive substances [11]. These vasoconstrictive or vasodilative factors mediate HSCs constriction or quiescence, altering the diameter of sinusoids to mediate the changes in hemodynamics [1]. For example, nitric oxide (NO) is assumed as a major vasodilative factor in liver to induce HSC quiescence [41]. LSECs yield high content of endothelial nitric oxide synthase (eNOS) and serve as the main source of NO [42]. Indeed, NO release is enhanced when LSECs are exposed to flow, implying that eNOS in LSECs is mechanosensitive to shear stress. Furthermore, a transcription factor Kruppel-like factor 2 (KLF2) is able to upregulate multiple vasoprotective genes including eNOS and NO in LSECs, which is also flow-dependent [43]. Another vasoprotective gene targeting KLF2 by shear stress is thrombomodulin (TM), a molecule that activates protein C via interacting with thrombin to prevent thrombosis [44]. Flow-induced increase of KLF2 in LSECs upregulates TM expression by binding to its promoter, suggesting an antithrombotic pathway in liver [45] (Fig. 3). In chronic liver diseases such as hepatic fibrosis and cirrhosis, however, LSECs no longer maintain HSC quiescence via NO-dependent pathway and lose their modulation of liver hemodynamics [1]. In these cases, LSECs yield a capillarized instead of differentiated phenotype, losing their fenestrae and growing basement membranes. In capillarized LSECs, the increase of shear stress fails to enhance NO expression but leads to vasoconstriction, so-called LSEC dysfunction [9, 21]. Collectively, LSECs regulate HSCs to control vascular tone

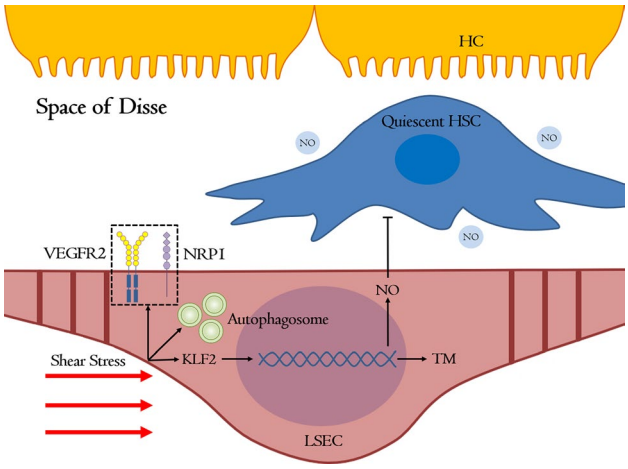

Fig. 3 Shear stress on LSECs. Blood flow initiates a series of mechanical signaling beneficial to LSECs. Shear stress upregulates Kruppel-like factor 2 (KLF2) and its downstream vasoprotective genes including nitric oxide (NO) [1] and thrombomodulin (TM). NO released by LSECs keeps HSCs quiescent and TM inhibits thrombosis formation. Under shear stress, autophagy in LSECs is activated. Besides, vascular endothelial cell growth factor receptor 2 (VEGFR2) and neuropilin-1 (NRP1) are translocated to plasma membrane and might be functional in liver regeneration after hepatectomy

in a KLF2-NO dependent pathway while de-differentiated LSECs lose this ability.

Partial hepatectomy is considered to be the gold standard operation to treat liver tumor, always followed by an increase in portal flow per gram in tissue [46]. The increased flow enhances the shear stress exerted on LSECs [47]. Vascular endothelial cell growth factor receptor 2 (VEGFR2) and neuropilin-1 (NRP1) in LSECs are translocated from perinuclear or faint cytoplasmic distribution to plasma membrane or cytoskeleton localization, with increased expression under physiological flow [48] (Fig. 3). In addition, inhibitor of DNA binding 1 (Id1), a member of helix–loop–helix (HLH) transcriptional factors which participates in cellular differentiation, proliferation and migration [49, 50], is demonstrated to be essential for VEGFR2 pathway and the Id1-VEGFR2 axis in LSECs leads to a rise in Wnt2 and HGF, contributing to liver regeneration after hepatectomy [51]. Notably, excessive hepatectomy induces undue shear stress and causes injury to LSECs. In a rat model of 90% hepatectomy, LSECs are disrupted with the disappearance of sieve plates and the space of Disse collapses one hour after surgery. These events lead to chaos in hepatic microcirculation [52]. Besides, portal hypertension induced by PH is also observed with the enlarged fenestrae on LSECs and the disturbed arrangement of sieve plates, presumably resulting in lipid accumulation in hepatocytes [53]. When liver samples are cultured on a rotational radial flow bioreactor at 0 revolutions per minute (RPM) (no shear stress), 30 RPM (moderate shear stress), and 120 RPM (high shear stress), respectively, large pores are presented on LSECs at 0 and 120 RPM, but not 30 RPM, implying that severe destruction of sinusoidal structures happens under improper shear stress and the liver may benefit from a proper moderate shear stress application [54]. Meanwhile, applying portal vein embolization (PVE) to swine before 90% hepatectomy protects the liver by maintaining stable hepatic hemodynamics with a much lower portal pressure and also improves liver functions [55]. A porto-caval shunt after transplantation of a swine model also decreases portal hypertension and protects the primary structures of sinusoids [56]. These results also suggest that physiological flow may benefit LSECs while excessive shear stress will damage them.

Liver ischemia-reperfusion (I/R) lesion contains hepatic interruption of blood flow (ischemia) and subsequent reperfusion, a common procedure in clinical operations like PH, liver transplantation and others, which results in liver damage and failure [57]. Effects of I/R are believed to be biphasic, *that is*, both hypoxia and lack of biomechanical stimuli contribute to liver injury after regaining oxygen and shear stress [58]. LSECs are considered the first to be injured [59] and existing evidence mostly focuses on I/R-induced LSECs damage due to hypoxia-reoxygenation and cold storage, but not flow cessation-restoration [18]. Over the past decade, machine-based perfusion in donor livers helps to maintain LSECs function and provide possibility of high-quality grafts [60, 61], implying that the shear stress probably plays a role in liver I/R. Interestingly, pulmonary endothelial cells can also sense the cessation of blood flow and activate downstream mechanotransduction during lung ischemia, which leads to production of reactive oxygen species (ROS) [62]. These observations give a hint that it might be LESCs that transduce shear stress during hepatic I/R and effects of shear stress on LSECs could play an important role in I/R injury.

Autophagy is an intracellular recycling system by degrading or reusing organelles and proteins and remaining homeostasis especially under harmful stimulations. In liver, laminar shear stress can activate autophagy of LSECs in vitro [63], supporting that normothermic machine perfusion prevents the liver from damage by stimulating the autophagy in LSECs [64]. These observations suggest that the flow-dependent autophagy helps to revert I/R liver injury (Fig. 3).

Shear stress also regulates cell adhesion to LSECs inside liver sinusoids. For example, engrafting cells like hepatocytes and other stem cells is a potential therapy for hepatic injury. Since LSECs are the gatekeeper in liver, these transplanted cells need to adhere to LSECs and then transmigrate across the endothelium. With shear stress increase from 0.03 dyne/cm^2 to 0.3 dyne/cm^2, the attaching number of perfused human liver stem cells decreases for about 80% [65]. By contrast, stimulating LSECs with TNF-α/IFN-γ demonstrates that the number of adherent lymphocytes goes up

with increased shear stress [66]. Thus, elucidating the roles of LSECs in cell adhesion under shear flow is also helpful to develop novel therapies.

3 Mechanical stretch on LSECs

3.1 Physical principles

The blood pressure exerts on sinusoids which are compliant and anisotropic, eliciting the pulsatile deformation including stretch and compression [67]. Because of the radial distension by diastolic and systolic pressures, this cyclic stretch on LSECs mediates various functions such as cell proliferation and differentiation or production of paracrine factors [68]. It is originated from cardiac cycle and usually coupled with blood perfusion inside the sinusoid in both directions parallel to and perpendicular to blood flow (Fig. 2). This mechanical stretch is usually defined by its strain and cyclic period when applied to LSECs in vitro. As the cyclic stretch is proved to be crucial in endothelium by participating in the release of vasoactive endothelial autacoids and other factors [67], it is likely that mechanical stretch may also play a role in LSECs functions.

3.2 Mechanical stretch measurements

To date there are no accurate standards to directly measure the mechanical stretch on LSECs in vivo. Since the stretch is derived from the pulsatile blood flow and the tensile strain denotes the increment in length per unit length, it could be inferred that the alteration of sinusoidal diameter may reflect the change of LSEC stretch [30]. During PH, the vessel diameter raises with the increased blood perfusion, implying the enhancement of cyclic stretch [20]. Besides, along with the development of fibrosis, activated HSCs contracts hepatic blood vessels and decreases sinusoidal diameter when angiogenesis happens, fueling the speculation that the circumferential tension on LSECs is altered in liver fibrosis and portal hypertension [23]. Unfortunately, no direct measurements are available in dealing with stretching LSECs at this stage.

3.3 Responses to mechanical stretch

Compared to shear stress, little has been known for the effects of mechanical stretch on hepatic sinusoids in vivo. Only a few works are attempted to understand the stretch-induced responses for isolated LSECs in vitro. To explore the roles of stretch on liver endothelium in portal hypertension, primary LSECs isolated from mice are subjected to cyclic biaxial stretch for 4 h at a strain of 20% and a frequency of 1 Hz. Microarray screening indicates that multiple cytokines are upregulated, among which CXCL1 is proved to induce neutrophil chemotaxis in vitro and LSECs could serve as the major source of CXCL1 in liver under physiological condition [69]. To examine the effect of upregulated CXCL1 by stretching LSECs in vivo, a mouse model of partial inferior vena cava ligation (pIVCL) is established to mimic a congestive hepatopathy (CH). It turns out that the progress of CH initiates the recruitment of neutrophils and accumulation of platelets through CXCL1 secretion, leading to formation of neutrophil extracellular traps (NETs) and thrombosis and promoting portal hypertension and fibrosis [69, 70]. Besides, gene network analysis from stretched LSECs uncovers the upregulation related to integrin signaling, calcium metabolism as well as Notch pathway [69]. Together with the data of human umbilical vein endothelial cells (HUVECs) on Notch pathway, conclusion is drawn that, under mechanical stretch, integrins on LSECs interact with Piezo channels and activate Notch pathway, thus raise sinusoidal CXCL1 to induce portal hypertension in CH [69] (Fig. 4). Therefore, mechanical stretch on LSECs stimulates secretion of CXCL1 to promote NETs formation in vivo.

Besides, mechanical stretch acting on LSECs participates in the regulation of liver regeneration in vitro. When LSECs derived from normal human liver tissue are loaded with uniaxial cyclic stretch at 50% strain, 1 Hz for 6-48 h, majority of the cells are elongated for about 150% along stretch direction and IL-6 expression in supernatants is improved [72]. This is meaningful for liver regeneration since IL-6 is known to be essential in proliferation [73] and recruit hepatocytes into cell cycling to quickly restore liver mass [74]. Besides, when PVE is applied to patients to embolize their right portal vein with fibrin glue, the diameters of the portal branches are increased immediately after PVE, as expected, suggesting that these hepatic vasculatures are exposed to circumferential stress. This process is followed by an increase of IL-6 in serum, consistent with those in vitro [72]. On the other hand, mechanical stretch on LSECs is able to induce angiocrine signals to support liver survival and growth in development, perfusion and PH. When human LSECs are loaded on a stretch chamber up to 20% strain for 1.5 h to mimic the vascular lumen widening, the cells are again elongated and both β1 integrin and vascular endothelial cell growth factor receptor 3 (VEGFR3) are activated with the enhanced interplay between the two proteins. Meanwhile, hepatocyte growth factor (HGF), IL-6, TNF-α and activated matrix metalloproteinase-9 (MMP9), which are assumed to participate liver regeneration [74–76], are all significantly upregulated (Fig. 4). These observations are further confirmed by ex vivo or in vivo tests. The embryos isolated from *Itgb1*-deficient mice are lack of β1 integrin and fail to activate VEGFR3 with increased blood flow when the embryos are treated with epinephrine for accelerating heart rate and enhancing blood perfusion in liver. Besides, after applying an open,

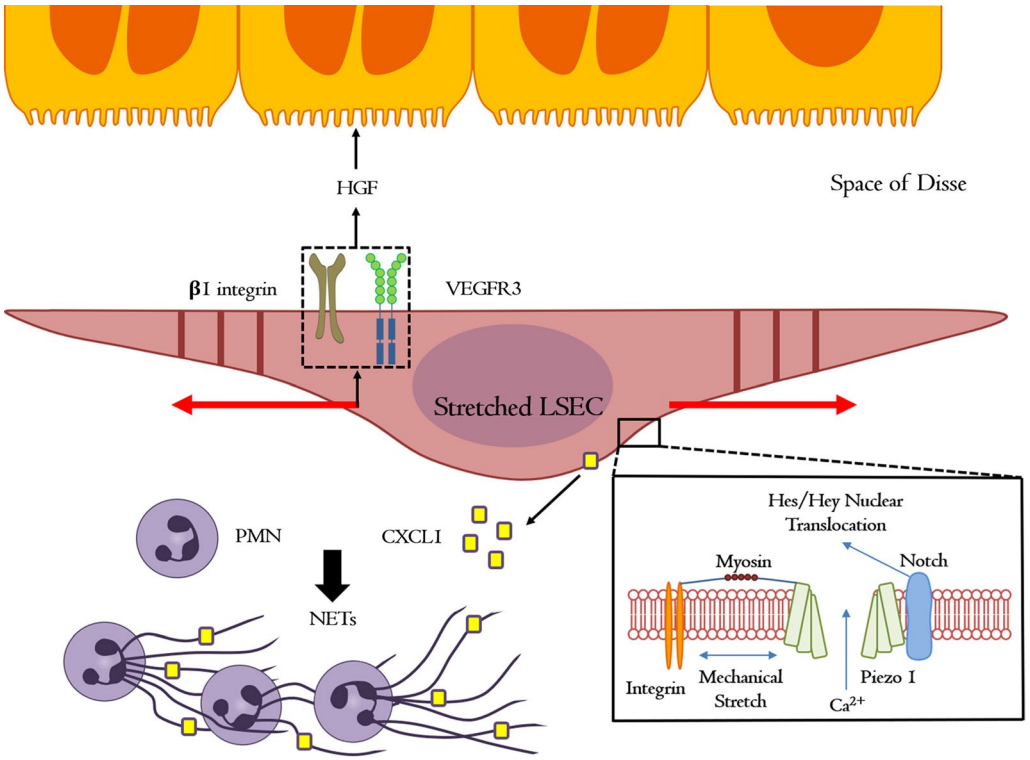

Fig. 4 Mechanical stretch on LSECs. Under mechanical stretch, integrin on LSECs interacts with Piezo 1 and activates Notch pathway to produce large amount of CXCL1, which promotes the formation of neutrophil extracellular traps (NETs) with neutrophils [69, 71]. The stretch also activates β1 integrin and vascular endothelial cell growth factor receptor 3 (VEGFR3) on LSECs and secrete angiocrine molecules to stimulate proliferation of HCs

non-recirculating perfusion to mouse liver by cannulating catheters in portal vein and inferior vena cava, much wider sinusoids are observed with enhanced activated endothelial β1 integrins [20]. These results imply that appropriate stretch on LSECs participates in liver regeneration.

Since shear stress and mechanical stretch are both induced by blood flow in vasculature, it is difficult to decouple the effects of the two in vivo. For a two-thirds PH, sinusoidal dilation appears, suggesting a change in stretch stress, and flow velocity is increased, implying a change in shear stress [20]. Thus, either the loss or the gain of blood perfusion in liver is more likely to be a superposed effect of both shear stress and mechanical stretch.

4 Substrate Stiffness on LSECs

4.1 Physical principles

The stiffness, also known as rigidity, is defined mechanically to describe the extent to which a substratum can resist deformation in response to applied forces. It is related to substratum modulus, loading condition and specimen geometry in concern. When it comes to biology, the stiffness is usually simplified as the modulus and refers to the collective biomechanical features of a specific tissue or ECM (Fig. 2) [16, 77]. This simplification that the stiffness could be presented by the modules only stands at the given loading condition and specimen geometry. For linear elastic materials within the elastic limit, Young's modulus is defined in units of pascals (Pa), by

$$E = \frac{\sigma}{\varepsilon}, \tag{2}$$

in which σ stands for stress and ε for strain. The higher E value is, the stiffer subject will be. Additionally, there are other parameters to characterize the stiffness, such as shear modulus (G) and bulk modulus (K), which are defined as

$$G = \frac{\tau}{\gamma}, \tag{3}$$

$$K = \frac{-\mathrm{d}p}{\mathrm{d}V/V}, \tag{4}$$

where the τ stands for shear stress, γ for shear strain, dp for the change of pressure and dV for the change of volume. Here the shear modulus defines the ability of a material

to resist transverse deformations while the bulk modulus deciphers the ability of a material to withstand changes in volume when placed under compression on all sides. Moreover, the two parameters of storage modulus (G') and loss modulus (G'') are also applied to describe the responses of a viscoelasticity material to stress or strain. Storage modulus is defined by the slope of the loading curve which is analogous to Young's modulus in a tensile test. It is a measure of how much energy must be input into the sample in order to distort it. Accordingly, the difference between the loading and unloading curves is called the loss modulus. It measures the energy lost during cyclic strain. Thus, stiffness is a key mechanical cue when dealing with LESCs functions in liver fibrosis or cirrhosis with highly enhanced stiffness of liver tissues.

4.2 Substrate stiffness measurements

The stiffness of the liver, as a viscoelastic tissue, varies significantly when suffering from distinct fibrotic stages and has gradually been accepted as a potential biomarker to characterize and evaluate the degree of liver fibrosis [16]. It is initiated with estimating the elastic features of the liver and promoted to determine its viscoelastic characteristics in recent years, by applying various techniques.

Ultrasound-based technique of transient elastography (UTE) is firstly introduced into liver in 2003 [78] and serves as a noninvasive approach to quantify the soft biological tissue stiffness in vivo [79]. This assay contains a probe of a low-frequency vibrator, a dedicated electronic system and a control unit. It works by a manageable transient shear wave with a servo-controlled vibration at given frequency and amplitude. Considering liver as a nonviscous, isotropic and soft elastic medium in a first approximation, the liver stiffness, E, is calculated as

$$E = 3\rho V_s^2, \tag{5}$$

where ρ is the mass density and V_s is the shear velocity. Technical limitations are still existing in UTE, mainly lying in the possible interference by other external factors such as increased waist circumference of patients as well as in the simplified elastic model (Eq. (2)) for a viscoelastic organ (liver), thus affecting its accuracy [78].

Acoustic radiation force impulse imaging (ARFI) is used to test liver stiffness in 2008 [80], also serving as a noninvasive assay to estimate local variations in tissue mechanics [81]. In ARFI, short-duration acoustic radiation forces are applied to generate localized displacements in a specified liver and these displacements are tracked spatially and temporally by ultrasound-related methods. Thus two-dimensional (2D) or 3D images of tissue displacement are built up [82] and the displacement magnitude is inversely proportional to the liver stiffness [83]. To date, applying the real-time ARFI still faces challenges in data acquisition, processing power and others [82].

Magnetic resonance elastography (MRE) has been widely used in liver to test stiffness since 1995 [84]. MRE assay is based on magnetic resonance imaging to quantify the mechanical properties of biological tissues in vivo. In MRE, mechanical shear waves are used, which propagate more rapidly in stiff tissue than soft one. Thus, the higher stiffness is reflected by the longer wavelength. By imaging these waves with a special MRI sequence and putting them into elastograms, the stiffness in liver can be quantitatively determined [85]. It is worth noting that there are still inapplicable cases with MRE assay, as seen for those patients who suffer from moderate to severe iron overload, where MRE signals might be too low to work [86].

Atomic force microscopy (AFM) is efficient when measuring a microscale region of localized liver to present the in situ stiffness perceived by a single cell. This assay is widely used to characterize the topographical and mechanical properties of biological materials. It works on force-indentation curves obtained from depth-sensing systems [6, 87, 88] and the Young's modulus, E, can be extracted from deflection-position data [89]. In a commonly used Hertz model, the Young's modulus is calculated as

$$E = \frac{3F(1-\nu^2)}{4\sqrt{R}\delta^{3/2}}, \tag{6}$$

where F is the applied force, ν is the Possion ratio, R is the radius of spherical probe and δ is the indentation depth [90]. It should be pointed out that, as the liver is viscoelastic, the adhesion force generated on contact surfaces, when indenting, will reduce the sensitivity and accuracy of measurement [91]. Although a few measurements based on a viscoelastic model are set up for AFM tests, they have not been used in liver specimens yet [92].

The liver stiffness has been quantified by different techniques for multiple species. For example, the shear storage modulus is tested by rheometry to be about 400 Pa in healthy rat liver and 1.2–1.4 kPa in fibrotic rat liver [24]. In mice, the stiffness measured by transient micro-elastography is about 3.6 ± 1.2 kPa in healthy liver while the Young's modulus is about 18.2 ± 3.7 kPa for the fibrotic one [93]. When measured by AFM, the stiffness of healthy liver tissue in mice is around 150 Pa and rises to 1–6 kPa in fibrotic models [90]. In human beings, the shear modulus is usually measured by MRE. At 60 Hz, it is to be < 2.5 kPa in healthy human liver and > 2.93 kPa at fibrosis stage or between 2.5 and 2.93 kPa in normal or inflammatory human liver [94].

4.3 Responses to substrate stiffness

When dealing with the effects of substrate stiffness on LSECs, we usually refer the *substrate* to the ECM that is mainly composed of collagen, elastin, fibronectin and other proteins [16] and believed to be a dynamic structure in liver microenvironment. For example, ECM scaffolds are able to be purified from hepatitis C virus (HCV)-infected patients at different stages of liver fibrosis and all the collagen deposition, elastin and fibronectin components are enhanced with the development of fibrosis [95]. By contrast, in CCl_4-induced fibrosis rat models, liver stiffness is increased before collagen deposition, suggesting that the collagen deposition may not contribute much to tissue stiffness at early fibrotic stages where the complete recovery could occur [24]. In Elastica van Gieson (EVG)-stained liver biopsy tissue specimens of chronic viral hepatitis patients, median area ratios of collagen and elastic fibers are positively correlated with liver stiffness [96]. On the other hand, ECM cross-linking is regarded as an important factor to enhance liver stiffness [97]. Lysyl oxidase (LOX) and transglutaminase (TG) are two major enzyme families in fibrotic progress [16]. Using LOXL2-specific inhibitor AB0023 in CCl_4-induced murine fibrosis, liver fibrosis could be rescued to the METAVIR F1 state, a degree of portal fibrosis without septa, indicating that inhibiting LOXL2 could reduce liver stiffness [98].

As mentioned above, LSECs can keep HSCs in quiescent state via KLF2-NO pathway and maintain a relatively thin ECM under physiological conditions. When the liver turns to be fibrotic, the capillarized LSECs release profibrogenic molecules, such as TGF-β, Hedgehog, laminin and fibronectin, to activate HSCs. These activated HSCs then start to proliferate, contract and produce excessive ECM components like collagens to induce fibrosis and further alter liver stiffness [9, 10]. When LSECs are placed in vitro on substrates with distinct stiffness, the phenotypic changes of LSECs are observed in response to the stiffness of collagen hydrogels with two moduli of 6 and 36 kPa that mimic the stiffness found in a healthy and fibrotic liver, respectively. The immortalized human LSECs on 6 kPa for 24 h exhibit well-defined fenestrae arranged in sieve plate structures, consist with those healthy cells and do not de-differentiate into pseudocapillarization state until 96 h later. In contrast, the human LSECs on 36 kPa lose fenestrae structure as early as 24 h. Additionally, CD31, a platelet endothelial cell adhesion molecule marked on the surface of de-differentiated or diseased LSECs, is not appeared for human LSECs on 6 kPa after 24 h but presented at 96 h. Moreover, CD31 is highly expressed in the cells on 36 kPa after 24 h, indicating the increase of substrate stiffness could promote the dedifferentiation of LSECs [99] (Fig. 5).

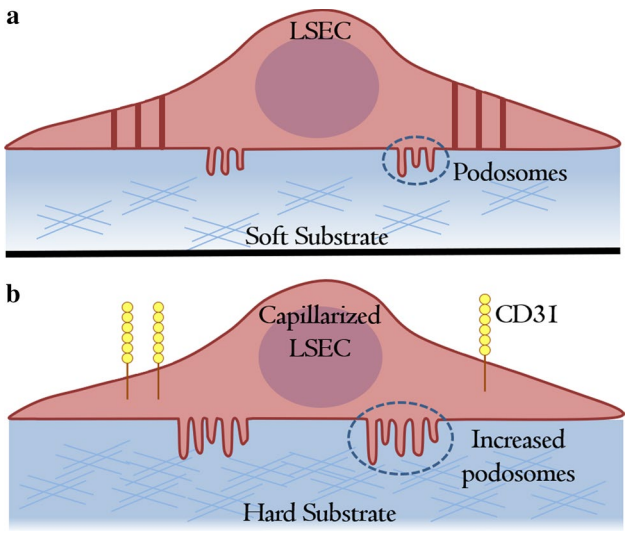

Fig. 5 Stiffness on LSECs. With increased ECM stiffness, LSECs gradually lose their differentiated phenotype. Fenestrae tend to disappear and CD31 molecules start to reoccur. The number and diameter of podosomes are also raised with substrate stiffening

On the other hand, human LSECs on a 36-kPa substrate present higher focal adhesion area and larger total area in morphology than those on 6 kPa. When isolated murine LSECs are placed on polyacrylamide gels at a stiffness of 1.75, 2, 2.25 and 20 kPa, respectively, the actin cytoskeleton is reorganized with enhanced cell spread as the stiffness is increased. Besides, the podosomes, an actin-based structure related to cell adhesion, migration, invasion and ECM degradation, are detected on primary LSECs and enhanced stiffness induces the increased number of podosomes [100]. Since the normal mouse liver stiffness is believed to be < 6 kPa while the F4 cirrhotic liver is > 12.5 kPa [93], this experiment nicely simulates the environment of normal and cirrhotic livers. These results suggest that podosomes participate in the ECM remodeling during fibrosis [100] (Fig. 5).

It is also noted that the regulation of substrate stiffness on LSECs could be bidirectional. When human LSECs are cultured on substrates with different stiffness from 90 Pa to 1.2 MPa or on coverslip to explore the angiogenesis during fibrosis, only those seeded on 200-600 Pa substrate could migrate to form capillary-like structures, a feature of angiogenesis in early hepatic fibrosis. In contrast, the cells on harder substrates above 1.2 kPa tend to migrate randomly and copy the features of leaky sinusoids at late stage of liver fibrosis [101]. Taken together, ECM stiffness is a key cue to dominate the differentiated or de-differentiated phenotype of LESCs via the related mechanosensitive pathways.

5 Potential mechanosensitive molecules on LSECs

Mechanical signaling in LSECs can orchestrate complex responses across the related cell types in liver sinusoids when LSECs sense the surrounding microenvironment such as blood flow, ECM and others. It seems reasonable to draw attention to those potential mechanosensitive molecules expressed on LSECs, even though evidence may be lacked at present to prove that they are directly regulated by mechanical forces. And those well-known mechanosensitive molecules, like integrin and Piezo 1 [71], are no longer discussed here.

5.1 Hedgehog

Hedgehog (Hh) pathway is a conserved morphogenic signaling that mediates cell cycle and differentiation and mainly contains three members, Sonic (Shh), Indian (Ihh), and Desert hedgehog [102–105]. Hh signaling also plays a key role in mechanotransductive responses. Shh is proved to be an osteogenic signal activated by mechanical stress and regulate osteoblastic differentiation. In mechanical unloading of bone marrow stromal cells (BMSCs), Shh signaling is down-regulated via DNA hypermethylation by binding to DNA methyltransferase 3b (Dnmt3b). Application of cyclic stretch at 0.5 Hz, 10% elongation reduces Dnmt3b expression, thus stimulates Hh signaling with osteoblastogenesis [106]. Ihh is required for chondrocyte proliferation when chondrocytes are cultured in 3D collagen sponge and subjected to 1 Hz, 5% elongation, where Ihh is activated to promote cell proliferation in a bone morphogenic protein (BMP)-dependent pattern. And inhibition of Ihh abolishes the effect of mechanical loading [107]. Thus, Ihh is sensitive to the tensile stress from matrix deformation and acts as an autocrine signal to stimulate chondrocyte proliferation [107]. By contrast, external mechanical stimuli can also weaken Hh signaling. To mimic the pulsatile flow, adult rat vascular smooth muscle cells (SMCs) are subjected to equibiaxial cyclic strain (10% stretch, 1 Hz). A dramatic decrease is visualized in Hh signaling with reduced proliferation and enhanced apoptosis [108]. These opposite effects imply that the responses to mechanical forces by Hh signaling may vary with different cell types. Besides, the cilium is mechanosensitive to trigger cell responses by mechanical stress in tissues like the kidney, liver, endothelium and bone [109], and Hh signaling plays an essential role in primary cilium [110, 111]. It can be assumed that external forces exerted on LSECs, like blood flow, may affect the cilium and then regulate its Hh pathway.

Hh signaling is proved to function in LSECs. Primary isolated LSECs produce both Hh ligands and receptors [112–114]. Cultured LSECs isolated from rats in vitro undergo the time-lapsed capillarization, with lost fenestrae, downregulated eNOS and VEGFR, and upregulated iNOS. Activation of Hh signaling is accompanied in the process and occurs before the first evidence of capillarization, suggesting that the active Hh signaling may initiate capillarization of LSECs. Inhibiting Hh pathway in capillarized LSECs could partially reverse the cells back to the healthy phenotype and prevent further capillarization both in vivo and in vitro [112]. In CCl_4-induced fibrosis model, liver X receptor α (LXRα) is upregulated and inhibits Hh pathway to abate the dedifferentiation of LSECs. Knockout of LXRα can further aggravate LSEC dedifferentiation and liver fibrosis [115]. Furthermore, Hh pathway regulates LSEC angiogenesis by transactivation of PROX1 and hypoxia inducible factor 1α (HIF-1α). The angiogenesis by Hh signaling can be inhibited by Curcumol, a natural anti-fibrotic medicine extracted from *Rhizoma Curcumae* [116].

5.2 Notch

Notch is a transmembrane protein and the Notch pathway serves as a conserved signaling which plays an important role in cellular development [117, 118]. The activation of Notch pathway requires the binding of its ligand to the Notch receptor and initiates proteolytic cleavages on the juxtamembrane region and then the transmembrane domain, releasing a Notch extracellular domain (NECD) and a Notch intracellular domain (NICD), respectively [119–121]. This process is believed to ask for a pulling force up to 12 pN. This force is generated by the ligand endocytosis with NECD and helps to expose the proteolysis site on Notch receptor for NICD [122], suggesting that the alterations in cellular tension may contribute to the Notch activation. It is known that Notch1 signaling is increased under laminar flow and its localization is polarized by shear stress in aortic endothelium. Moreover, the nuclear NICD level is raised when shear stress increases [123]. The NICD so produced is able to translocate into nucleus for transcriptional regulation [120], indicating that laminar flow could activate the Notch pathway. These clues not only signify that shear force promotes the progress of Notch cleavage, but also proves that Notch is directly, highly and positively sensitive to mechanical stimuli such as shear stress, serving as mechanosensor on endothelium.

Additionally, Notch signaling is believed to be critical for LSECs. Notch proteins are expressed by endothelial cells including LSECs [124]. Deletion of endothelial Notch or Rbpj1, a canonical effector of Notch, results in severe disruption of sinusoidal architecture in immature mice and lead to liver necrosis. Deleting endothelial Rbpj1 in adult

mice induces sinusoidal dilation, vascular shunts or portal hypertension. Besides, the lack of Rbpj1 alters the morphology of LSECs. These isolated Rbpj-KO LSECs exhibit an increasing number of membranous "holes", abnormal from the healthy ones [125]. Thus, appropriate Notch signaling in LSECs is required for development and maintenance of hepatic vascular structure and function. On the other hand, over-activation of Notch pathway in LSECs disrupts homeostasis. Notch activation leads to the decreased fenestrae and increased basement membrane, inducing the dedifferentiation of LSECs. This activation also inhibits the eNOS/soluble guanylate cyclase (sGC) signaling, interrupting the reverse of LSEC dedifferentiation and attenuating hepatocyte proliferation [126]. Moreover, DLL4, a ligand of the Notch signaling pathway, is overexpressed in human LSECs and CCl_4-induced murine fibrotic livers, resulting in producing basement membrane proteins. DLL4 silencing in vivo helps to reduce LSEC capillarization, confirming that over-activation of Notch signaling harms LSECs and liver homeostasis [127].

5.3 YAP

Yes-associated protein (YAP), known as a transcription coactivator paired with multiple transcription factors and also an effector of Hippo tumor-suppressor pathway, regulates senescence, chemoresistance, proliferation and angiogenesis [128–130]. YAP is believed to be closely related to the underlying mechanotransduction [131, 132]. YAP and the transcriptional coactivator with PDZ-binding motif, TAZ, serve as the downstream factors to sense cells' physical microenvironment. In mammary epithelial cells (MECs), the activity of YAP/TAZ on stiff hydrogels is much higher than that on soft matrix, with more YAP/TAZ located in nuclear rather than cytoplasmic regions [131]. In mesenchymal stem cells (MSCs) and human lung microvascular endothelial cells (HMVECs), the localization of YAZ/TAZ is altered from nuclear to cytoplasmic regions when the single cells are cultured on the defined micropatterns to confine its spreading. Besides, YAP/TAZ of MSCs remains to stay in nuclear regions on micropillars, suggesting that YAP/TAZ are regulated by cell geometry imposed by ECM [131]. Furthermore, it is indicated that YAP/TAZ activity relies on the small GTPase Rho and formation of stress fibers, two of which are activated by cell spreading. Meanwhile, nuclear localization of YAP/TAZ requires cytoskeleton tension generated by ROCK and non-muscle myosin when cells respond to ECM [131]. In a word, ECM stiffness and cell geometry direct cell fate by regulating YAP/TAZ activity and, in turn, the external mechanical stimulation can be counteracted by adjusting the activity of YAP/TAZ [131]. Except for substrate stiffness, YAP also responses to blood flow as well. In living zebrafish, YAP1 can enter into nucleus and promote the followed transcriptions via F-actin reorganization under blood flow. In cultured human endothelial cells, the exposure of laminar shear stress also helps YAP nuclear translocation, confirming the positive relationship between YAP activation and blood flow [133]. Besides, YAP has been proved to be necessary for endothelial cell proliferation in response to mechanical stretch [134].

Meanwhile, YAP is expressed on LSECs and functions in liver angiogenesis during fibrosis. Oroxylin A, a natural active component extracted from *Scutellariae* radix, is proved to inhibit hypoxia-induced nuclear translocation of YAP in primary isolated LSECs and then attenuate the accumulation of HIF-1α. As a result, the downstream genes such as *VEGF-A* and *Ang-2* are down-regulated, leading to anti-angiogenesis [129].

5.4 Filamentous actin

The actin cytoskeleton is a dynamic network of polar filaments. It is also a major part of cell cortex that serves as the scaffold to support the cell and respond to extracellular physical stimuli [135, 136]. Filamentous actin (F-actin), also known as actin filaments, is the core of the cytoskeleton network [137]. Different kinetics happen at both ends of F-actin, where a nucleotide hydrolysis takes place at one end and a faster polymerization is presented at the other [138]. F-actin mediates multiple cellular processes such as cell adhesion, migration and division. As the stress fibers in cells, F-actin plays an indispensable role in mechanotransmission and mechanotransduction [139]. The dynamic assembly of F-actin controls the cell shape and force generation [140].

F-actin sustains the morphology of LSECs and preserves the formation of fenestrae. When culturing LSECs in vitro, F-actin is found to surround fenestrae within sieve plates and form the specialized structure that stabilizes the membrane and supports the fenestrae [141]. Meanwhile, newly-formed sieve plates are observed immediately after incubating cytochalasin B with LSECs to de-polymerize F-actin and further expanded with time in increased number of fenestrae, confirming that F-actin regulated the size and number of fenestrae in a time-dependent manner [142]. In addition, iodoacetic acid (IAA) is also used to interrupt the polymerization of F-action. Since F-actin is known to support the membrane-bound pores together with spectrin, adding IAA destabilizes the actin-spectrin scaffold in LSECs and thus enhances the number of fenestrae in a relatively long period. In this case, fenestrae are quickly switched between open and close states [143]. Another related regulator is Rho, a ras-related GTP-binding protein that stimulates the formation of stress fibers [144]. Treating isolated rat LSECs with lysophosphatidic acid (LPA) is

able to active Rho, which in turn induces the contraction of fenestrae along with formation of dense thick actin stress fibers. In contrast, inhibiting Rho by C3-transferase dilates the fenestrae and fuses them to form large pores, mainly attributed to disassembly of stress fibers [145]. Thus, F-actin is assumed to support and mediate the dynamic changes of fenestrae, probably via a Rho-related way.

6 Remarks and perspectives

LSECs reside in a dynamic mechanical microenvironment in liver sinusoids. Like other endothelial cells, LSECs are sensitive and responsive to external mechanical stimuli in proper ways. Typical shear stress, mechanical stretch and substrate stiffness exerted on LSECs, as discussed above, initiate a series of biomechanical signaling, in which LSECs act as a mechanical sensor and regulator. And for clarity,

Table 1 Summary of mechanotransduction under typical mechanical stimuli on LSECs

Stimuli	Pattern	Parameters	Acting cells/tissues	Testing indexes	References
Perfusion (shear stress/stretch)	*Ex vivo* mouse liver perfusion	4–8 ml min^{-1}	Mouse liver	Activated β1 integrin (on LSECs)	Lorenz et al. [20]
		2–8 ml min^{-1}	Mouse liver	p-VEGFR3(on LSECs)	
	ex vivo human liver perfusion	7 mmHg for portal, 70–80 mmHg for hepatic artery, 60–180 min	Human liver	KLF2, eNOS or TM mRNA (in LSECs)	Beijert et al. [146]
		7 mmHg for portal, 70–80 mmHg for hepatic artery, 180 min	Human liver	Nitric oxide concentration	
Stretch	Cyclic biaxial stretch	20%, 1 Hz, 4 h	Primary murine LSEC	Microarray (including CXCL1)	Hilscher et al. [69]
	Uniaxial stretch	20%, 1.5 h	Primary human LSEC	Length, activated β1 integrin, VEGFR3 *p*-tyr, HGF, IL-6, TNF-α	Lorenz et al. [20]
	Uniaxial stretch	50%, 1 Hz, 6/12/24/48 h	Primary human LSEC	Length, IL-6, HGF, TNF-α	Kawai et al. [72]
Shear stress	Laminar flow	20 dyn/cm^2, 24 h	TSEC	Autophagy	Hammoutene et al. [63]
		14.1 dyn/cm^2, 30 min	Primary rat LSEC	KLF2, eNOS or TM mRNA	Marrone et al. [45]
		0.03–0.3 dyn/cm^2, 24 h	Primary rat LSEC	Attached human liver stem cells	Noh et al. [65]
		0.5–1 dyn/cm^2	Primary human LSEC	Rolling lymphocytes on LSEC	Shetty et al. [66]
		14.1 dyn/cm^2, 12 h	Primary rat LSEC	KLF2 mRNA	Gracia-Sancho et al. [43]
		14.1 dyn/cm^2, 30 min	Primary rat LSEC	NO_x	Shah et al. [42]
Stiffness	Stiffness (2D)	90 Pa to 1.2 MPa, 5/10/20 h	Primary human LSEC	Capillary-like structures forming	Liu et al. [101]
		6 kPa, 24–96 h; 36 kPa, 24 h	Primary human LSEC	Fenestrae diameter, fenestrae density, focal adhesion area, focal adhesion number	Ford et al. [99]
		6 kPa, 36 kPa	Primary human LSEC	Area	
		6 kPa, 96 h; 36 kPa, 96 h	Primary human LSEC	Cell proliferation	
		6 kPa, 24–96 h; 36 kPa, 24–96 h	Primary human LSEC	VEGF	
		1.75–20 kPa, 24 h	Primary mouse LSEC	LSECs with podosome (%)	Juin et al. [100]
		2–20 kPa, 24 h	Primary mouse LSEC	podosome diameter	

detailed mechanical parameters related to LSECs in the literatures are summarized in Table 1.

Continuous physiological flow tends to be beneficial and necessary for LSECs, since the shear stress enhances the autophagy of LSECs [63] and contributes to liver regeneration via NO secretion [1] and Id1-VEGFR2 axis [51]. Similarly, mechanical stretch derived from embryonic development or partial hepatectomy also promotes the regeneration via IL-6 upregulation [72] and HGF upregulation through β1 integrin and/or VEGFR3 activation [20], a crucial process involving cross-talk between LSECs and HCs [9, 147]. Improper blood flow disturbs the phenotype of LSECs and interrupts their functions, as exemplified that excessive shear stress injuries LSECs by ruining their morphology [52, 53] and interfering their secretion [54]. Abnormal stretch by CH or ligation of inferior vena cava leads to overexpression of CXCL1 on LSECs, accounting for the potential portal hypertension [69]. Substrate stiffness on which LSECs are placed are tightly associated with their morphology and functions. With collagen deposition and cross-linking in the space of Disse, high ECM stiffness increases the number of podosomes and mediates the cytoskeleton reorganization of LSECs [100]. Only a moderate (but not high or low) stiffness can promote the formation of capillary-like structures, implying the bidirectional effects of substrate stiffness [101]. This process turns to be more complicated when LSECs and HSCs constitute a positive feedback regulation on stiffness [9].

Morphological changes and functional alterations of LSECs exposed to mechanical stimuli are governed by their mechanotransductive signaling. Fenestrae structure of LSECs serve as the golden readout of their differentiated phenotype. Capillarized LSECs with fenestrae disappearance fail to regulate the HSCs' behaviors and lose the control of vascular tone or ECM production [1]. Several signaling molecules, Hh, Notch, YAP, and F-actin, are known to be mechanosensitive and also required for maintaining the phenotype and functions of LSECs. Laminar flow activates Notch signaling and enhances NICD nuclear level in aortic endothelium [123]. Similarly, laminar or blood flow promotes YAP nuclear translocation both in living zebrafish and cultured human endothelial cells [133]. The Hh signaling pathway induced by mechanical stretch varies with cell types. Mechanical stretch activates Hh pathway in BMSCs and chondrocytes to stimulate osteoblastogenesis and chondrocyte proliferation [106, 107]. In SMCs, however, the stretch weakens Hh signaling and reduces proliferation [108]. ECM stiffness regulates YAP/TAZ activity and their subcellular localization. In MECs, stiff substrates enhance YAP/TAZ activity and promote their nuclear localization while soft substrates present the opposite effects [131]. F-actin, as an essential component of cytoskeleton, supports the formation of LSEC fenestrae in a time-dependent manner [141, 142]. De-polymerize F-actin increases number of fenestrae [142]. It is thus reasonable to presume that these molecules serve as the candidates for LSECs and play a role in response to mechanical stimuli. Due to the advantages of mechanotransduction that lie in longer transmission range and slower signal decay rate [16], it is clear that the mechanical sensitivity in LSECs is indispensable in elucidating liver homeostasis and fibrosis or even cirrhosis.

Mechanical effects on LSECs also anticipates that the regulation of mechanical microenvironment is a potential strategy in treating liver diseases. For example, portal vein shunt, splenectomy and splenic artery embolization can be used to reduce blood flow in liver and then prevent liver failure [1, 16]. Besides, vasodilative drugs such as olprinone are functional in decreasing blood perfusion after surgery, also protecting liver from surgical damage [1].

Several issues remain challenging in terms of the effects of mechanical stimuli on LSECs. First, in vivo mechanical parameters remain to be determined quantitatively for human or animal species. New techniques are required to measure accurately the sinusoidal geometry and the blood flow velocity inside sinusoids. And more realistic 3D models are needed to provide reliable forecasts on sinusoidal parameters when techniques have not been improved yet. Viscoelastic modeling is also necessarily developed to predict ECM elasticity, combined with UTE and MRE measurements. Second, the roles of shear stress and mechanical stretch in regulating LSEC functions are usually coupled together in vivo. In vitro isolation of the two factors may be a simplified approach to decouple their respective contributions, but it still needs to know how to integrate those in vitro data with in vivo functions. Third, LESC fenestrae evolution dynamics is known to be critical in their capillarization and thus liver fibrosis or cirrhosis, and the underlying mechanisms remain unclear especially under varied mechanical stimuli. More mechanosensitive molecules need to be screened and their mechanotransductive signaling should be deciphered.

Acknowledgements This work was supported by the National Natural Science Foundation of China (Grants 91642203, 31627804, and 31870930), the Scientific Instrument Developing Project, Strategic Priority Research Program and Frontier Science Key Project of Chinese Academy of Sciences (Grants GJJSTU20190005, QYZDJ-SSW-JSC018 and XDB22040101).

References

1. Poisson, J., Lemoinne, S., Boulanger, C., et al.: Liver sinusoidal endothelial cells: Physiology and role in liver diseases. J. Hepatol. **66**(1), 212–227 (2017)
2. Maslak, E., Gregorius, A., Chlopicki, S.: Liver sinusoidal endothelial cells (LSECs) function and NAFLD; NO-based

therapy targeted to the liver. Pharmacol. Rep. **67**(4), 689–694 (2015)
3. DeLeve, L.D.: Vascular liver disease and the liver sinusoidal endothelial cell. In: DeLeve, L.D., Garcia-Tsao, G. (eds.) Vascular Liver Disease: Mechanisms and Management. Springer, New York (2011)
4. Wisse, E.: An electron microscopic study of fenestrated endothelial lining of rat liver sinusoids. J. Ultrastruct. Res. **31**(1), 125–150 (1970)
5. Braet, F., Wisse, E.: Structural and functional aspects of liver sinusoidal endothelial cell fenestrae: a review. Comp. Hepatol. **1**(1), 1 (2002)
6. Li, P.W., Zhou, J., Li, W., et al.: Characterizing liver sinusoidal endothelial cell fenestrae on soft substrates upon AFM imaging and deep learning. Biochim. Biophys. Acta Gen. Subj. **1864**(12), 129702 (2020).
7. Wisse, E., De Zanger, R.B., Charels, K., et al.: The liver sieve—considerations concerning the structure and function of endothelial fenestrae, the sinusoidal wall and the space of Disse. Hepatology **5**(4), 683–692 (1985)
8. Shetty, S., Lalor, P.F., Adams, D.H.: Liver sinusoidal endothelial cells—gatekeepers of hepatic immunity. Nat. Rev. Gastroenterol. Hepatol. **15**(9), 555–567 (2018)
9. Marrone, G., Shah, V.H., Gracia-Sancho, J.: Sinusoidal communication in liver fibrosis and regeneration. J. Hepatol. **65**(3), 608–617 (2016)
10. Hammoutene, A., Rautou, P.: Role of liver sinusoidal endothelial cells in non-alcoholic fatty liver disease. J.. Hepatol. **70**(6), 1278–1291 (2019)
11. Vollmar, B., Menger, M.D.: The hepatic microcirculation: mechanistic contributions and therapeutic targets in liver injury and repair. Physiol. Rev. **89**(4), 1269–1339 (2009)
12. Schaffner, F., Popper, H.: Capillarization of hepatic sinusoids in man. Gastroenterology. **44**(3), 239–242 (1963)
13. Urashima, S., Tsutsumi, M., Nakase, K., et al.: Studies on capillarization of the hepatic sinusoids in alcoholic liver-disease. Alcohol Alcohol Suppl. **28**(1B), 77–84 (1993)
14. Xu, B., Broome, U., Uzunel, M., et al.: Capillarization of hepatic sinusoid by liver endothelial cell-reactive autoantibodies in patients with cirrhosis and chronic hepatitis. Am. J. Pathol. **163**(4), 1275–1289 (2003)
15. DeLeve, L.D.: Liver sinusoidal endothelial cells in hepatic fibrosis. Hepatology. **61**(5), 1740–1746 (2015)
16. You, Z.F., Zhou, L., Li, W.J., et al.: Mechanical microenvironment as a key cellular regulator in the liver. Acta Mech. Sin. **35**(2), 289–298 (2019)
17. Eipel, C., Abshagen, K., Vollmar, B.: Regulation of hepatic blood flow: the hepatic arterial buffer response revisited. World J. Gastroenterol. **16**(48), 6046–6057 (2010)
18. Grande Nakazato, P.C., Victorino, J.P., Fina, C.F., et al.: Liver ischemia and reperfusion injury. Pathophysiology and new horizons in preconditioning and therapy. Acta Cir. Bras. **33**(8), 723–735 (2018)
19. Golse, N., Bucur, P.O., Adam, R., et al.: New paradigms in post-hepatectomy liver failure. J. Gastrointest. Surg. **17**(3), 593–605 (2013)
20. Lorenz, L., Axnick, J., Buschmann, T., et al.: Mechanosensing by beta 1 integrin induces angiocrine signals for liver growth and survival. Nature **562**(7725), 128–132 (2018)
21. DeLeve, L.D., Wang, X.D., Guo, Y.M.: Sinusoidal endothelial cells prevent rat stellate cell activation and promote reversion to quiescence. Hepatology **48**(3), 920–930 (2008)
22. Garcia-Pagan, J.C., Gracia-Sancho, J., Bosch, J.: Functional aspects on the pathophysiology of portal hypertension in cirrhosis. J. Hepatol. **57**(2), 458–461 (2012)
23. Thabut, D., Shah, V.: Intrahepatic angiogenesis and sinusoidal remodeling in chronic liver disease: new targets for the treatment of portal hypertension? J. Hepatol. **53**(5), 976–980 (2010)
24. Georges, P.C., Hui, J.J., Gombos, Z., et al.: Increased stiffness of the rat liver precedes matrix deposition: implications for fibrosis. Am. J. Physiol. Gastrointest. Liver Physiol. **293**(6), G1147–G1154 (2007)
25. Ajmera, V.H., Liu, A., Singh, S., et al.: Clinical utility of an increase in magnetic resonance elastography in predicting fibrosis progression in nonalcoholic fatty liver disease. Hepatology **71**(3), 849–860 (2020)
26. Xing, X., Yan, Y.L., Shen, Y., et al.: Liver fibrosis with two-dimensional shear-wave elastography in patients with autoimmune hepatitis. Expert Rev. Gastroenterol. Hepatol. **14**(7), 631–638 (2020)
27. Higuchi, M., Tamaki, N., Kurosaki, M., et al: Changes of liver stiffness measured by magnetic resonance elastography during direct-acting antivirals treatment in patients with chronic hepatitis C. J. Med. Virol. Online ahead of print
28. Medrano, L.M., Garcia-Broncano, P., Berenguer, J., et al.: Elevated liver stiffness is linked to increased biomarkers of inflammation and immune activation in HIV/hepatitis C virus-coinfected patients. AIDS **32**(9), 1095–1105 (2018)
29. Ko, B.J., Kim, Y.S., Kim, S.G., et al.: Relationship between 25-hydroxyvitamin d levels and liver fibrosis as assessed by transient elastography in patients with chronic liver disease. Gut Liver. **10**(5), 818–825 (2016)
30. Davies, P.F.: Flow-mediated endothelial mechanotransduction. Physiol. Rev. **75**(3), 519–560 (1995)
31. Ballermann, B.J., Dardik, A., Eng, E., et al.: Shear stress and the endothelium. Kidney Int. **54**, S100–S108 (1998)
32. Johnson, F.P.: The development of the lobule of the pig's liver. Am. J. Anat. **25**(3), 299–331 (1919)
33. Deal, C.P., Green, H.D.: Comparison of changes in mesenteric resistance following splanchnic nerve stimulation with responses to epinephrine and norepinephrine. Circ. Res. **4**(1), 38–44 (1956)
34. Wen, B., Liang, J., Deng, X., et al.: Effect of fluid shear stress on portal vein remodeling in a rat model of portal hypertension. Gastroenterol. Res. Pract. **41**, 1–7 (2015)
35. Aghasafari, P., Pidaparti, R.: Influence of tidal-volume setting, emphysema and ARDS on human alveolar sacs mechanics. Acta Mech. Sin. **34**(5), 983–993 (2018)
36. Liu, Z.M., Zhao, S.W., Li, Y.J., et al.: Influence of coronary bifurcation angle on atherosclerosis. Acta Mech. Sin. **35**(6), 1269–1278 (2019)
37. Debbaut, C., Vierendeels, J., Casteleyn, C., et al.: Perfusion characteristics of the human hepatic microcirculation based on three-dimensional reconstructions and computational fluid dynamic analysis. J. Biomech. Eng. **134**(1), 011003 (2012)
38. Wei, W., Pu, Y.S., Wang, X.K., et al.: Wall shear stress in portal vein of cirrhotic patients with portal hypertension. World J. Gastroenterol. **23**(18), 3279–3286 (2017)
39. Peeters, G., Debbaut, C., Cornillie, P., et al.: A multilevel modeling framework to study hepatic perfusion characteristics in case of liver cirrhosis. J. Biomech. Eng. **137**(5), 051007 (2015)
40. Hu, J.R., Lu, S.Q., Feng, S.L., et al.: Flow dynamics analyses of pathophysiological liver lobules using porous media theory. Acta Mech. Sin. **33**(4), 823–832 (2017)
41. Fernandez, M.: Molecular pathophysiology of portal hypertension. Hepatology **61**(4), 1406–1415 (2015)
42. Shah, V., Haddad, F.G., Garcia-Cardena, G., et al.: Liver sinusoidal endothelial cells are responsible for nitric oxide modulation of resistance in the hepatic sinusoids. J. Clin. Invest. **100**(11), 2923–2930 (1997)
43. Gracia-Sancho, J., Russo, L., Garcia-Caldero, H., et al.: Endothelial expression of transcription factor Kruppel-like

factor 2 and its vasoprotective target genes in the normal and cirrhotic rat liver. Gut **60**(4), 517–524 (2011)
44. Conway, E.M.: Thrombomodulin and its role in inflammation. Semin. Immunopathol. **34**(1), 107–125 (2012)
45. Marrone, G., Russo, L., Rosado, E., et al.: The transcription factor KLF2 mediates hepatic endothelial protection and paracrine endothelial-stellate cell deactivation induced by statins. J. Hepatol. **58**(1), 98–103 (2013)
46. Garcea, G., Maddern, G.J.: Liver failure after major hepatic resection. J. Hepato-Biliary Pancreatic Surg. **16**(2), 145–155 (2009)
47. Schoen, J.M., Wang, H.H., Minuk, G.Y., et al.: Shear stress-induced nitric oxide release triggers the liver regeneration cascade. Nitric Oxide **5**(5), 453–464 (2001)
48. Braet, F., Shleper, M., Paizi, M., et al.: Liver sinusoidal endothelial cell modulation upon resection and shear stress in vitro. Comp. Hepatol. **3**(1), 7 (2004)
49. Kim, H.J., Chung, H., Yoo, Y.G., et al.: Inhibitor of DNA binding 1 activates vascular endothelial growth factor through enhancing the stability and activity of hypoxia-inducible factor-1 alpha. Mol. Cancer Res. **5**(4), 321–329 (2007)
50. Wang, H., Yu, Y., Guo, R.W., et al.: Inhibitor of DNA binding-1 promotes the migration and proliferation of endothelial progenitor cells in vitro. Mol. Cell. Biochem. **335**(1–2), 19–27 (2010)
51. Ding, B.S., Nolan, D.J., Butler, J.M., et al.: Inductive angiocrine signals from sinusoidal endothelium are required for liver regeneration. Nature **468**(7321), 310–315 (2010)
52. Yamanaka, K., Hatano, E., Narita, M., et al.: Olprinone attenuates excessive shear stress through up-regulation of endothelial nitric oxide synthase in a rat excessive hepatectomy model. Liver Transplant. **17**(1), 60–69 (2011)
53. Morsiani, E., Mazzoni, M., Aleotti, A., et al.: Increased sinusoidal wall permeability and liver fatty change after two-thirds hepatectomy: an ultrastructural study in the rat. Hepatology **21**(2), 539–544 (1995)
54. Torii, T., Miyazawa, M., Koyama, I.: Effect of continuous application of shear stress on liver tissue: continuous application of appropriate shear stress has advantage in protection of liver tissue. Transpl. Proc. **37**(10), 4575–4578 (2005)
55. Asencio, J.M., Garcia-Sabrido, J.L., Lopez-Baena, J.A., et al.: Preconditioning by portal vein embolization modulates hepatic hemodynamics and improves liver function in pigs with extended hepatectomy. Surgery **161**(6), 1489–1501 (2017)
56. Asakura, T., Ohkohchi, N., Orii, T., et al.: Portal vein pressure is the key for successful liver transplantation of an extremely small graft in the pig model. Transpl. Int. **16**(6), 376–382 (2003)
57. Lentsch, A.B., Kato, A., Yoshidome, H., et al.: Inflammatory mechanisms and therapeutic strategies for warm hepatic ischemia/reperfusion injury. Hepatology **32**(2), 169–173 (2000)
58. Peralta, C., Jimenez-Castro, M.B., Gracia-Sancho, J.: Hepatic ischemia and reperfusion injury: Effects on the liver sinusoidal milieu. J. Hepatol. **59**(5), 1094–1106 (2013)
59. Huet, P.M., Nagaoka, M.R., Desbiens, G., et al.: Sinusoidal endothelial cell and hepatocyte death following cold ischemia-warm reperfusion of the rat liver. Hepatology **39**(4), 1110–1119 (2004)
60. Garcia-Valdecasas, J.C., Fondevila, C.: In-vivo normothermic recirculation: an update. Curr. Opin. Org. Transpl. **15**(2), 173–176 (2010)
61. Xue, S., He, W.Y., Zeng, X.P., et al.: Hypothermic machine perfusion attenuates ischemia/reperfusion injury against rat livers donated after cardiac death by activating the Keap1/Nrf2-ARE signaling pathway. Mol. Med. Rep. **18**(1), 815–826 (2018)
62. Chatterjee, S., Nieman, G.F., Christie, J.D., et al.: Shear stress-related mechanosignaling with lung ischemia: lessons from basic research can inform lung transplantation. Am. J. Physiol. Lung Cell. Mol. Physiol. **307**(9), L668–L680 (2014)
63. Hammoutene, A., Biquard, L., Lasselin, J., et al.: A defect in endothelial autophagy occurs in patients with non-alcoholic steatohepatitis and promotes inflammation and fibrosis. J. Hepatol **72**(3), 528–538 (2020)
64. Boteon, Y.L., Laing, R., Mergental, H., et al.: Mechanisms of autophagy activation in endothelial cell and their targeting during normothermic machine liver perfusion. World J. Gastroenterol. **23**(48), 8443–8451 (2017)
65. Noh, J.K., Jung, J.G., Jang, E.M., et al.: Live cell-imaging perfusion culture system of liver sinusoidal endothelial cells to mimic stem cell engraftment in liver. Transpl. Proc. **44**(4), 1116–1119 (2012)
66. Shetty, S., Weston, C.J., Oo, Y.H., et al.: Common lymphatic endothelial and vascular endothelial receptor-1 mediates the transmigration of regulatory T cells across human hepatic sinusoidal endothelium. J. Immunol. **186**(7), 4147–4155 (2011)
67. Busse, R., Fleming, I.: Pulsatile stretch and shear stress: physical stimuli determining the production of endothelium-derived relaxing factors. J. Vasc. Res. **35**(2), 73–84 (1998)
68. Rabbany, S.Y., Ding, B.S., Larroche, C., et al.: Mechanosensory pathways in angiocrine mediated tissue regeneration. In: Gefen, A., Aviv, R. (eds.) Studies in Mechanobiology, Tissue Engineering and Biomaterials. Springer, Berlin, Heidelberg, New York (2013)
69. Hilscher, M.B., Sehrawat, T., Arab, J.P., et al.: Mechanical stretch increases expression of CXCL1 in liver sinusoidal endothelial cells to recruit neutrophils, generate sinusoidal microthombi, and promote portal hypertension. Gastroenterology. **157**(1), 193–209 (2019)
70. Wanless, I.R., Liu, J.J., Butany, J.: Role of thrombosis in the pathogenesis of congestive hepatic-fibrosis (cardiac cirrhosis). Hepatology. **21**(5), 1232–1237 (1995)
71. Soydemir, S., Comella, O., Abdelmottaleb, D., et al.: Does mechanocrine signaling by liver sinusoidal endothelial cells offer new opportunities for the development of anti-fibrotics? Front. Med. **6**, 312 (2020)
72. Kawai, M., Naruse, K., Komatsu, S., et al.: Mechanical stress-dependent secretion of interleukin 6 by endothelial cells after portal vein embolization: clinical and experimental studies. J. Hepatol. **37**(2), 240–246 (2002)
73. Cressman, D.E., Greenbaum, L.E., DeAngelis, R.A., et al.: Liver failure and defective hepatocyte regeneration in interleukin-6-deficient mice. Science **274**(5291), 1379–1383 (1996)
74. Sakamoto, T., Liu, Z.J., Murase, N., et al.: Mitosis and apoptosis in the liver of interleukin-6-deficient mice after partial hepatectomy. Hepatology **29**(2), 403–411 (1999)
75. Bohm, F., Kohler, U.A., Speicher, T., et al.: Regulation of liver regeneration by growth factors and cytokines. EMBO Mol. Med. **2**(8), 294–305 (2010)
76. Olle, E.W., Ren, X.D., McClintock, S.D., et al.: Matrix metalloproteinase-9 is an important factor in hepatic regeneration after partial hepatectomy in mice. Hepatology **44**(3), 540–549 (2006)
77. Handorf, A.M., Zhou, Y.X., Halanski, M.A., et al.: Tissue stiffness dictates development, homeostasis, and disease progression. Organogenesis **11**(1), 1–15 (2015)
78. Sandrin, L., Fourquet, B., Hasquenoph, J.M., et al.: Transient elastography: A new noninvasive method for assessment of hepatic fibrosis. Ultrasound Med. Biol. **29**(12), 1705–1713 (2003)
79. Mueller, S., Sandrin, L.: Liver stiffness: a novel parameter for the diagnosis of liver disease. Hepat. Med. **2**, 49–67 (2010)
80. Palmeri, M.L., Wang, M.H., Dahl, J.J., et al.: Quantifying hepatic shear modulus *in vivo* using acoustic radiation force. Ultrasound Med. Biol. **34**(4), 546–558 (2008)

81. Wegner, M., Iskender, E., Azzarok, A., et al.: Comparison of acoustic radiation force impulse imaging with the convex probe 6C1 and linear probe 9L4. Medicine (Baltimore). **99**(16), e19701 (2020)
82. Dahl, J.J., Pinton, G.F., Palmeri, M.L., et al.: A parallel tracking method for acoustic radiation force impulse imaging. IEEE Trans. Ultrason. Ferroelectr. Freq. Control **54**(2), 301–312 (2007)
83. Palmeri, M.L., Sharma, A.C., Bouchard, R.R., et al.: A finite-element method model of soft tissue response to impulsive acoustic radiation force. IEEE Trans. Ultrason. Ferroelectr. Freq. Control **52**(10), 1699–1712 (2005)
84. Muthupillai, R., Lomas, D.J., Rossman, P.J., et al.: Magnetic-resonance elastography by direct visualization of propagating acoustic strain waves. Science **269**(5232), 1854–1857 (1995)
85. Venkatesh, S.K., Yin, M., Ehman, R.L.: Magnetic resonance elastography of liver: technique, analysis, and clinical applications. J. Magn. Reson. Imaging **37**, 544–555 (2013)
86. Taouli, B., Ehman, R.L., Reeder, S.B.: Advanced MRI methods for assessment of chronic liver disease. AJR Am. J .Roentgenol. **193**(1), 14–27 (2009)
87. Gang, Z., Qi, Q., Jing, C., et al.: Measuring microenvironment mechanical stress of rat liver during diethylnitrosamine induced hepatocarcinogenesis by atomic force microscope. Microsc. Res. Tech. **72**(9), 672–678 (2009)
88. Hu, J.R., Huang, D.D., Zhang, Y., et al.: Global mapping of live cell mechanical features using PeakForce QNM AFM. Biophys. Rep. **6**(1), 9–18 (2020)
89. Lin, D.C., Dimitriadis, E.K., Horkay, F.: Advances in the mechanical characterization of soft materials by nanoindentation. Recent Res. Dev. Biophys. **5**, 333–370 (2006)
90. Desai, S.S., Tung, J.C., Zhou, V.X., et al.: Physiological ranges of matrix rigidity modulate primary mouse hepatocyte function in part through hepatocyte nuclear factor 4 alpha. Hepatology **64**(1), 261–275 (2016)
91. Butt, H.J., Jaschke, M., Ducker, W.: Measuring surface forces in aqueous-electrolyte solution with the atomic-force microscope. Bioelectrochem. Bioenerget. **38**(1), 191–201 (1995)
92. Efremov, Y.M., Okajima, T., Raman, A.: Measuring viscoelasticity of soft biological samples using atomic force microscopy. Soft Matter **16**(1), 64–81 (2020)
93. Bastard, C., Bosisio, M.R., Chabert, M., et al.: Transient microelastography: a novel non-invasive approach to measure liver stiffness in mice. World J. Gastroenterol. **17**(8), 968–975 (2011)
94. Hoodeshenas, S., Yin, M., Venkatesh, S.K.: Magnetic resonance elastography of liver: current update. Top. Magn. Reson. Imaging **27**(5), 319–333 (2018)
95. Baiocchini, A., Montaldo, C., Conigliaro, A., et al.: Extracellular matrix molecular remodeling in human liver fibrosis evolution. PLoS ONE **11**(3), e0151736 (2016)
96. Abe, T., Hashiguchi, A., Yamazaki, K., et al.: Quantification of collagen and elastic fibers using whole-slide images of liver biopsy specimens. Patho.l Int. **63**(6), 305–310 (2013)
97. Kolacna, L., Bakesova, J., Varga, F., et al.: Biochemical and biophysical aspects of collagen nanostructure in the extracellular matrix. Physiol. Res. **56**(Suppl 1), S51–S60 (2007)
98. Barry-Hamilton, V., Spangler, R., Marshall, D., et al.: Allosteric inhibition of lysyl oxidase-like-2 impedes the development of a pathologic microenvironment. Nat. Med. **16**(9), 1009–1017 (2010)
99. Ford, A.J., Jain, G., Rajagopalan, P.: Designing a fibrotic microenvironment to investigate changes in human liver sinusoidal endothelial cell function. Acta Biomater. **24**, 220–227 (2015)
100. Juin, A., Planus, E., Guillemot, F., et al.: Extracellular matrix rigidity controls podosome induction in microvascular endothelial cells. Biol. Cell **105**(1), 46–57 (2013)
101. Liu, L.W., You, Z.F., Yu, H.S., et al.: Mechanotransduction-modulated fibrotic microniches reveal the contribution of angiogenesis in liver fibrosis. Nat. Mater. **16**(12), 1252–1261 (2017)
102. Bok, J., Zenczak, C., Hwang, C.H., et al.: Auditory ganglion source of Sonic hedgehog regulates timing of cell cycle exit and differentiation of mammalian cochlear hair cells. Proc. Natl. Acad. Sci. USA **110**(34), 13869–13874 (2013)
103. Masai, I., Yamaguchi, M., Tonou-Fujimori, N., et al.: The hedgehog-PKA pathway regulates two distinct steps of the differentiation of retinal ganglion cells: the cell-cycle exit of retinoblasts and their neuronal maturation. Development **132**(7), 1539–1553 (2005)
104. Abramyan, J.: Hedgehog signaling and embryonic craniofacial disorders. J. Dev. Biol. **7**(2), 9 (2019)
105. Binder, M., Chmielarz, P., McKinnon, P.J., et al.: Functionally distinctive Ptch receptors establish multimodal Hedgehog signaling in the tooth epithelial stem cell niche. Stem Cells **37**(9), 1238–1248 (2019)
106. Wang, C.D., Shan, S.Z., Wang, C.L., et al.: Mechanical stimulation promote the osteogenic differentiation of bone marrow stromal cells through epigenetic regulation of Sonic Hedgehog. Exp. Cell. Res. **352**(2), 346–356 (2017)
107. Wu, Q.Q., Zhang, Y., Chen, Q.: Indian hedgehog is an essential component of mechanotransduction complex to stimulate chondrocyte proliferation. J. Biol. Chem. **276**(38), 35290–35296 (2001)
108. Morrow, D., Sweeney, C., Birney, Y.A., et al.: Biomechanical regulation of hedgehog signaling in vascular smooth muscle cells in vitro and in vivo. Am. J. Physiol. Cell Physiol. **292**(1), C488–C496 (2007)
109. Hoey, D.A., Downs, M.E., Jacobs, C.R.: The mechanics of the primary cilium: an intricate structure with complex function. J. Biomech. **45**(1), 17–26 (2012)
110. Corbit, K.C., Aanstad, P., Singla, V., et al.: Vertebrate Smoothened functions at the primary cilium. Nature **437**(7061), 1018–1021 (2005)
111. Kim, J., Kato, M., Beachy, P.A.: Gli2 trafficking links Hedgehog-dependent activation of Smoothened in the primary cilium to transcriptional activation in the nucleus. Proc. Natl. Acad. Sci. USA **106**(51), 21666–21671 (2009)
112. Xie, G.H., Choi, S.S., Syn, W.K., et al.: Hedgehog signalling regulates liver sinusoidal endothelial cell capillarization. Gut **62**(2), 299–309 (2013)
113. Pereira, T.D., Witek, R.P., Syn, W.K., et al.: Viral factors induce Hedgehog pathway activation in humans with viral hepatitis, cirrhosis, and hepatocellular carcinoma. Lab. Invest. **90**(12), 1690–1703 (2010)
114. Witek, R.P., Yang, L., Liu, R.S., et al.: Liver cell-derived microparticles activate hedgehog signaling and alter gene expression in hepatic endothelial cells. Gastroenterology **136**(1), 320–330 (2009)
115. Xing, Y., Zhao, T.T., Gao, X.Y., et al.: Liver X receptor alpha is essential for the capillarization of liver sinusoidal endothelial cells in liver injury. Sci. Rep. **6**, 11 (2016)
116. Yang, X., Wang, Z.M., Kai, J., et al.: Curcumol attenuates liver sinusoidal endothelial cell angiogenesis via regulating Glis-PROX1-HIF-1 alpha in liver fibrosis. Cell Prolif. **53**(3), 134–144 (2020)
117. Weinmaster, G., Fischer, J.A.: Notch ligand ubiquitylation: what is it good for? Dev. Cell. **21**(1), 134–44 (2011)
118. Henrique, D., Schweisguth, F.: Mechanisms of Notch signaling: a simple logic deployed in time and space. Development **146**(3), dev172148 (2019).
119. D'Souza, B., Miyamoto, A., Weinmaster, G.: The many facets of Notch ligands. Oncogene **27**(38), 5148–5167 (2008)

120. Kopan, R.: Notch Signaling. Cold Spring Harb. Perspect. Biol. **4**(10), a011213 (2012).
121. Shen, W., Sun, J.J.: Different modes of Notch activation and strength regulation in the spermathecal secretory lineage. Development **147**(3), dev184390 (2020).
122. Meloty-Kapella, L., Shergill, B., Kuon, J., et al.: Notch ligand endocytosis generates mechanical pulling force dependent on dynamin, epsins, and actin. Dev. Cell **22**(6), 1299–1312 (2012)
123. Mack, J.J., Mosqueiro, T.S., Archer, B.J., et al.: NOTCH1 is a mechanosensor in adult arteries. Nat. Commun. **8**(1), 1620 (2017)
124. Loomes, K.M., Taichman, D.B., Glover, C.L., et al.: Characterization of Notch receptor expression in the developing mammalian heart and liver. Am. J. Med. Genet. **112**(2), 181–189 (2002)
125. Cuervo, H., Nielsen, C.M., Simonetto, D.A., et al.: Endothelial Notch signaling is essential to prevent hepatic vascular malformations in mice. Hepatology **64**(4), 1302–1316 (2016)
126. Duan, J.-L., Ruan, B., Yan, X.-C., et al.: Endothelial Notch activation reshapes the angiocrine of sinusoidal endothelia to aggravate liver fibrosis and blunt regeneration in mice. Hepatology **68**(2), 677–690 (2018)
127. Chen, L.Y., Gu, T.Y., Li, B.H.: Delta-like ligand 4/DLL4 regulates the capillarization of liver sinusoidal endothelial cell and liver fibrogenesis. Biochim. Biophys. Acta Mol. Cell. Res. **1866**(10), 1663–1675 (2019)
128. Bai, H.B., Zhang, N.L., Xu, Y., et al.: Yes-associated protein regulates the hepatic response after bile duct ligation. Hepatology **56**(3), 1097–1107 (2012)
129. Zhang, C.X., Bian, M.L., Chen, X.R., et al.: Oroxylin A prevents angiogenesis of LSECs in liver fibrosis via inhibition of YAP/HIF-1 signaling. J. Cell. Biochem. **119**(2), 2258–2268 (2018)
130. Zheng, Y.G., Pan, D.J.: The Hippo signaling pathway in development and disease. Dev. Cell **50**(3), 264–282 (2019)
131. Dupont, S., Morsut, L., Aragona, M., et al.: Role of YAP/TAZ in mechanotransduction. Nature **474**(7350), 179–183 (2011)
132. Totaro, A., Panciera, T., Piccolo, S.: YAP/TAZ upstream signals and downstream responses. Nat. Cell. Biol. **20**(8), 888–899 (2018)
133. Nakajima, H., Yamamoto, K., Agarwala, S., et al.: Flow-dependent endothelial YAP regulation contributes to vessel maintenance. Dev. Cell **40**(6), 523–536 (2017)
134. Neto, F., Klaus-Bergmann, A., Ong, Y.T., et al.: YAP and TAZ regulate adherens junction dynamics and endothelial cell distribution during vascular development. eLife **7**, e31037 (2018).
135. Watanabe, N., Tohyama, K., Yamashiro, S.: Mechanostress resistance involving formin homology proteins: G- and F-actin homeostasis-driven filament nucleation and helical polymerization-mediated actin polymer stabilization. Biochem. Biophys. Res. Commun. **506**(2), 323–329 (2018)
136. Wang, Y.Z., Qian, J.: Buckling of filamentous actin bundles in filopodial protrusions. Acta Mech. Sin. **35**(2), 365–375 (2019)
137. Kadzik, R.S., Homa, K.E., Kovar, D.R.: F-actin cytoskeleton network self-organization through competition and cooperation. Annu. Rev. Cell. Dev. Biol. **36**, 35–60 (2020)
138. Merino, F., Pospich, S., Raunser, S.: Towards a structural understanding of the remodeling of the actin cytoskeleton. Semin. Cell. Dev. Biol. **102**, 51–64 (2020)
139. Sun, X.Y., Phua, D.Y.Z., Axiotakis, L.J., et al.: Mechanosensing through direct binding of tensed f-actin by LIM domains. Dev. Cell **55**(4), 468–482 (2020)
140. Stricker, J., Falzone, T., Gardel, M.L.: Mechanics of the F-actin cytoskeleton. J. Biomech. **43**(1), 9–14 (2010)
141. Monkemoller, V., Oie, C., Hubner, W., et al.: Multimodal super-resolution optical microscopy visualizes the close connection between membrane and the cytoskeleton in liver sinusoidal endothelial cell fenestrations. Sci. Rep. **5**, 16279 (2015).
142. Zapotoczny, B., Szafranska, K., Owczarczyk, K., et al.: Atomic force microscopy reveals the dynamic morphology of fenestrations in live liver sinusoidal endothelial cells. Sci. Rep. **7**(1), 7994 (2017)
143. Zapotoczny, B., Braet, F., Kus, E., et al.: Actin-spectrin scaffold supports open fenestrae in liver sinusoidal endothelial cells. Traffic **20**(12), 932–942 (2019)
144. Ridley, A.J., Hall, A.: The small GTP-binding protein rho regulates the assembly of focal adhesions and actin stress fibers in response to growth-factors. Cell **70**(3), 389–399 (1992)
145. Yokomori, H., Yoshimura, K., Funakoshi, S., et al.: Rho modulates hepatic sinusoidal endothelial fenestrae via regulation of the actin cytoskeleton in rat endothelial cells. Lab. Invest. **84**(7), 857–864 (2004)
146. Beijert, I., Mert, S., Huang, V., et al.: Endothelial dysfunction in steatotic human donor livers: a pilot study of the underlying mechanism during subnormothermic machine perfusion. Transpl. Direct **4**(5), e345 (2018)
147. Du, Y., Li, N., Yang, H., et al.: Mimicking liver sinusoidal structures and functions using a 3D-configured microfluidic chip. Lab. Chip **17**(5), 782–794 (2017)